Research on
Engineering
Structures & Materials
journal homepage: http://jresm.org

RESEARCH
GROUP

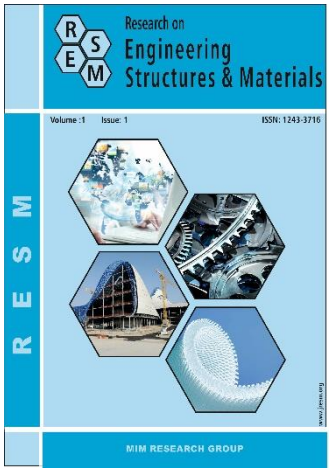

Model updating effects on the seismic behavior of tall buildings under far and near-fault ground motions

Betül Demirtaş, Alemdar Bayraktar, Aydın Dumanoğlu

Online Publication Date: 24 Nov 2016
URL: http://dx.doi.org/10.17515/resm2016.64st0719.html
DOI: http://dx.doi.org/10.17515/resm2016.64st0719

Journal Abbreviation: *Res. Eng. Struct. Mat.*

To cite this article
Demirtas B, Bayraktar A, Dumanoglu A. Model updating effects on the seismic behavior of tall buildings under far and near-fault ground motions. *Res. Eng. Struct. Mat*., 2017; 3(2): 99-112

Research on
Engineering
Structures & Materials
journal homepage: http://jresm.org

RESEARCH GROUP

Research Article

Model updating effects on the seismic behavior of tall buildings under far and near-fault ground motions

Betül Demirtaş*[1], Alemdar Bayraktar[1], Aydın Dumanoğlu[2]

[1] *Department of Civil Engineering, Karadeniz Technical University, Trabzon, Turkey*
[2] *Department of Civil Engineering, Canik Başarı University, Samsun, Turkey*

Article Info

Article history:
Received 19 Jul 2016
Revised 18 Nov 2016
Accepted 24 Nov 2016

Keywords:
Model updating,
Tall buildings,
Ambient vibration testing,
Near-fault ground motion,
Seismic behavior

Abstract

The study investigates ambient vibration based model updating effects on the seismic behavior of a RC tall building subjected to far and near-fault ground motions. A 17-storey building built in Giresun, Turkey is selected as an application. Firstly, 3D initial finite element model of the selected building is created and determined analytical dynamic characteristics. Then, experimental dynamic characteristics of the building (frequencies, mode shapes, damping ratios) are determined by Operational Modal Analysis Method using the ambient vibration test data. According to experimental results, initial finite element model is calibrated by using boundary conditions and material properties. Initial and calibrated finite element models of the building are analysed under far and near-fault ground motions. Two models are compared with each other in terms of displacement, velocity, acceleration, base bending moment, base shear force, compressive and tensile stresses.

1. Introduction

Nowadays, in developed and in developing countries, a considerable increase is observed in the construction of tall buildings. Safety evaluation of existing tall buildings to earthquake motions is very important. Dynamic characteristics such as natural frequencies, damping ratios and mode shapes are one of the most important parameters for the safety evaluation of tall buildings. Determining the change of modal parameters may help carried out to condition assessment of the structure or even damage detection in the process of construction or during its service life [1]. Acceleration data plays an important role, based on which modal parameters of the structures can be obtained [2-4]. The dynamic characteristics of engineering structures can be obtained by finite element method and experimental measurement methods. The most commonly used experimental measurement method is Operational Modal Analysis (OMA). In recent years, there has been an increasing interest in determination of dynamic characteristics of tall buildings by OMA. Ventura and Schuster [5], Wu and Li [6], Miyashita et al. [7], Xu and Zhan [8], Li et al. [9-12], Brownjohn et al. [13], Boroschek and Yáñez [14], Li and Yi [15], Liu et al. [16], Zang et al. [17] implemented full-scale measurements of tall buildings. Li and Wu [18] created seven 3D FE models of a 78-story super-tall building, and numerical results were compared with their field measurements to identify the modelling errors for the purpose of updating FE models. Pan et al. [19] presented numerical studies on dynamic responses of the tallest building in Singapore with correlation with their field measurements. Chassiakos et al. [20] performed a study on ambient vibration data collected before, during, and after the structural retrofitting. Archila et al. [21] conducted a modal test using ambient vibrations on a 22 story building repaired after the earthquake to determine its dynamic properties. Pan et al. [22]

*Correspondingauthor: betuldemirtas@ktu.edu.tr
DOI: http://dx.doi.org/10.17515/resm2016.64st0719

presented the signal processing results for a 128 storey building by using the Frequency Domain Decomposition and the Enhanced Frequency Domain Decomposition techniques. The most significant lateral and torsional mode shapes and associated periods of vibration were determined within the frequency range of 0.1–2 Hz.

Near-fault ground motions which expose the structure to high input energy in the beginning of the earthquake have the potential to cause a large response and considerable damage to structures [23]. Therefore, structural response to near-fault ground motions has received much attention in recent years. The effects of near-fault ground motions on civil engineering structures such as buildings and bridges, etc., have been investigated in many recent studies [24-29].

This paper aims to investigate the effects of ambient vibration based model updating on the seismic behaviour of a RC tall building subjected to far and near-fault ground motions. Firstly, the analytical dynamic characteristics are obtained by using the initial finite element model. Then experimental dynamic characteristics are extracted using Enhanced Frequency Domain Decomposition technique. Finite element model of the building is updated by changing of material properties and boundary conditions to eliminate the differences between analytical and experimental dynamic characteristics. Linear seismic behaviours of the building for both initial and updated finite element models are determined under the selected earthquake ground motions.

2. Formulation

The experimental dynamic characteristics of the structure were determined by Enhanced Frequency Domain Decomposition (EFDD) technique. In this technique, the natural frequencies, modal damping ratios and mode shapes were extracted from the power spectra by selecting peak values [30-32]. The relationship between the unknown input and the measured responses can be written as;

$$G_{yy}(j\omega)=H(j\omega)^{*}G_{xx}(j\omega)H(j\omega)^{T} \tag{1}$$

where G_{xx} is the Power Spectral Density (PSD) matrix of the input signal, G_{yy} is the PSD matrix of the output signal, H is the Frequency Response Function (FRF) matrix, and * and T denote complex conjugate and transpose, respectively [32]. The FRF can be written in partial fraction, i.e. pole/residue form;

$$H(j\omega)=\sum_{k=1}^{n}\frac{R_k}{j\omega-\lambda_k}+\frac{R_k^{*}}{j\omega-\lambda_k^{*}} \tag{2}$$

where n is the number of modes λ_k is the pole and, R_k is the residue [32]. Then Eq. (1) becomes as:

$$G_{yy}(j\omega)=\sum_{k=1}^{n}\sum_{s=1}^{n}\left[\frac{R_k}{j\omega-\lambda_k}+\frac{R_k^{*}}{j\omega-\lambda_k^{*}}\right]G_{xx}(j\omega)\left[\frac{R_s}{j\omega-\lambda_s}+\frac{R_s^{*}}{j\omega-\lambda_s^{*}}\right]^{\overline{H}} \tag{3}$$

where s is the singular values, superscript H denotes complex conjugate and transpose [32]. Multiplying the two partial fraction factors and making use of the Heaviside partial fraction theorem, after some mathematical manipulations, the output PSD can be reduced to a pole/residue form as fallows;

$$G_{yy}(j\omega)=\sum_{k=1}^{n}\frac{A_k}{j\omega-\lambda_k}+\frac{A_k^{*}}{j\omega-\lambda_k^{*}}+\frac{B_k}{-j\omega-\lambda_k}+\frac{B_k^{*}}{-j\omega-\lambda_k^{*}} \tag{4}$$

where Ak and B_k are the k-th residue matrices of the output PSD [32]. In the EFDD identification, the first step is to estimate the PSD matrix. The estimation of the output PSD known at discrete frequencies is then decomposed by taking the SVD of the matrix;

$$G_{yy}(j\omega_i)=U_i S_i U_i^{\bar{H}} \quad (5)$$

where the matrix $U_i=[u_{i1}, u_{i2},...,u_{im}]$ is a unitary matrix holding the singular vectors u_{ij}, and s_{ij} is a diagonal matrix holding the scalar singular values. The first singular vector u_{ij} is an estimation of the mode shape. PSD function is identified around the peak by comparing the mode shape estimation u_{ij} with the singular vectors for the frequency lines around the peak. From the piece of the SDOF density function obtained around the peak of the PSD, the natural frequency and the damping can be obtained [32].

3. Application

3.1. Description of the Selected Building

The seventeen-storey building that was constructed in Giresun, Turkey is one of the highest buildings in the city. It was built to be used as a residance. It has a rectangular plan, two basements, a ground floor, fourteen normal floors, and an attic. The height of the building is 47.6m and its dimensions are 20m x 30m. The floor height of the building is 2.8m. The building has a raft foundation. While performing measurement, all floors were built with brick walls. The view, plan and section of the building are given in Fig. 1.

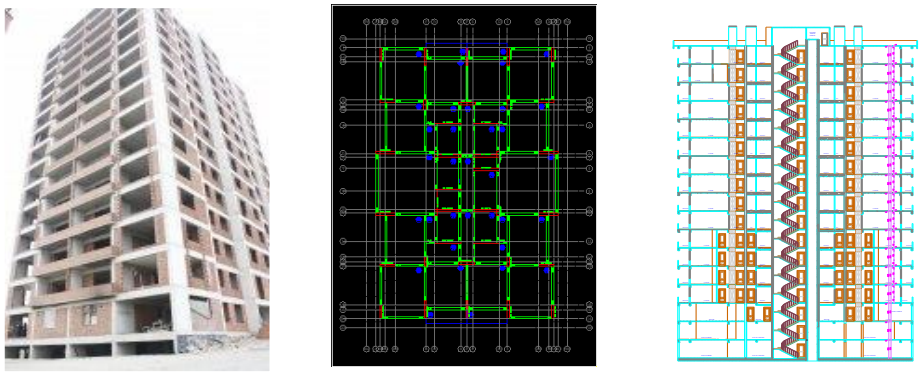

Fig. 1. The view, plan and section of the selected building

3.2. Theoretical Modal Analysis of the Building

Three-dimensional finite element model of the building was created by SAP2000 [33] program. The building was modelled by using plane and frame elements. The beams were modelled by the frame elements, and the shear walls and floors were modelled by the plane elements. 35053 joints, 4522 frames, and 41068 plane elements were used to model of the building. Firstly, all degrees of freedom under base of the building were assumed as fixed. The initial finite element model is given in Fig. 2.

Two different material properties were considered such as concrete and brick. The material properties assumed in the analyses are given in Table 1. The first three natural frequencies and mode shapes obtained from analytical modal analysis of the building are given in Fig. 3.

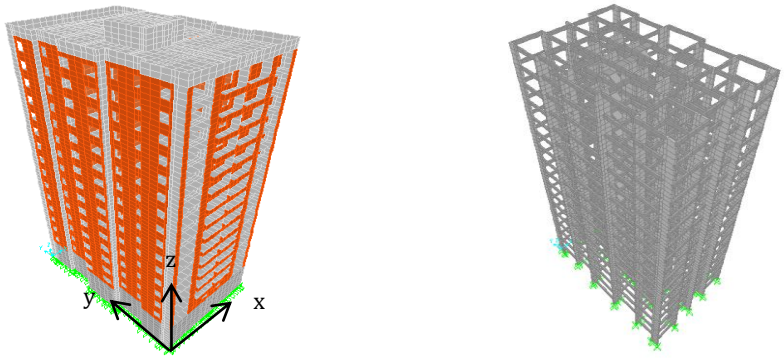

Fig. 2. The initial finite element model of the building

Table 1. Material properties used in theoretical modal analysis of the building

Material	Modulus of Elasticity (N/m^2)	Poisson Ratio	Density (kg/m^3)
Concrete	3.2E10	0.2	2450
Brick	3.2E9	0.2	1600

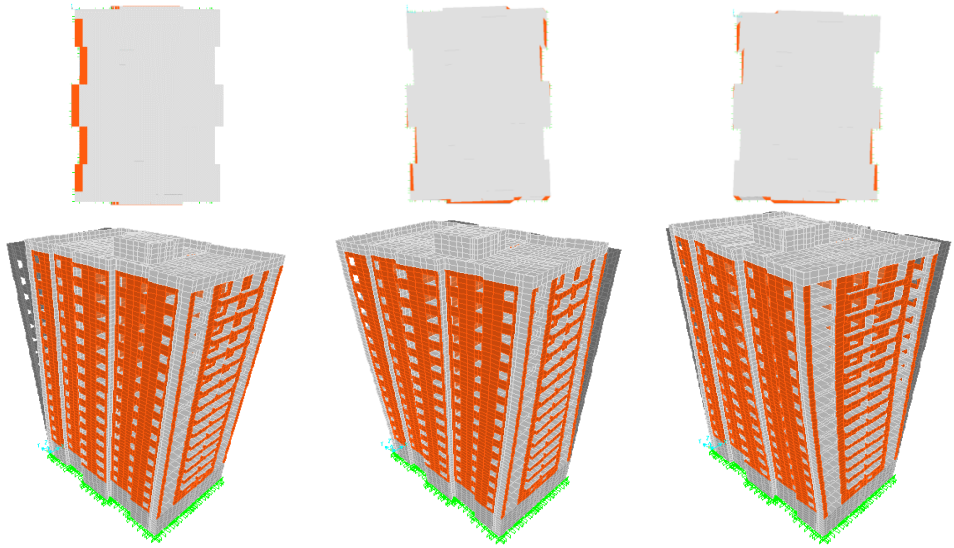

1st Mode (f_1=1.639Hz) 2nd Mode (f_2=1.819Hz) 3rd Mode (f_3=1.907Hz)

Fig. 3. The first three analytical mode shapes of the building

The first three analytical frequencies were obtained between 1-2 Hz. The first three mode shapes of the building were obtained as transverse mode, torsional mode and torsional mode, respectively.

3.3. Operational Modal Analyses of the Building

The dynamic characteristics obtained from the finite element model of the building give an idea on the dynamic behaviour of the building, but are not sufficient alone to determine the current behaviour of the building. For this reason, the results obtained

from finite element model of the building must be confirmed by the results obtained by experimental method. Accordingly, the full-scale vibration test of the building was conducted by Operational Modal Analysis (OMA) method under ambient vibrations. During the ambient measurements of the building, B&K 8340 type uni-axial accelerometers which have 10V/g sensitivity, B&K 3560 type data acquisition system with 17 channels, PULSE [34] and OMA [35] softwares were used.

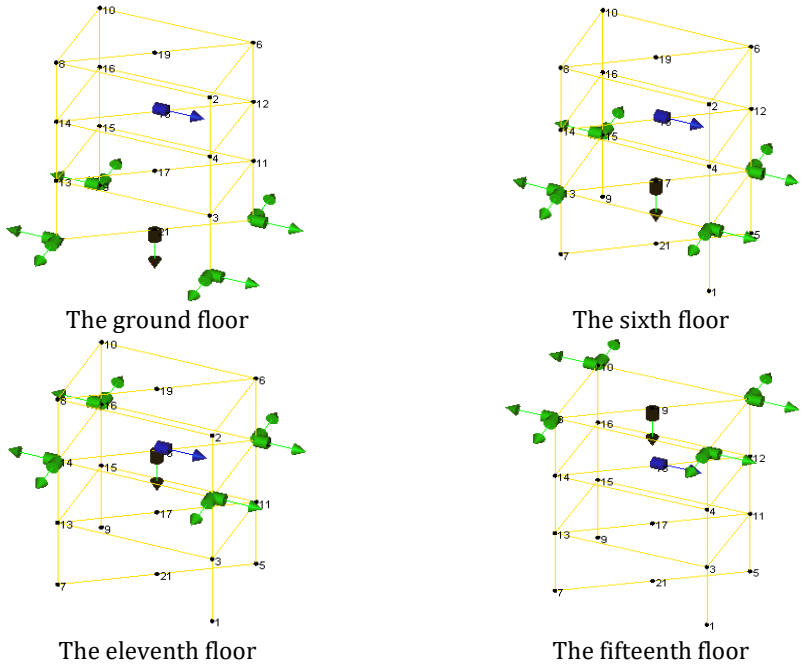

The ground floor

The sixth floor

The eleventh floor

The fifteenth floor

a) Measurement steps

b) Total measurement setup

Fig. 4. Total measurement setup and location of the accelerometers

The experimental dynamic behaviour of the building was determined by taking the measurements from different floor levels. Total four different measurements with a reference sensor were implemented. The measurements were taken from the ground floor, the sixth floor, the eleventh floor and the fifteenth floor, which is attic. And the eleventh floor was selected as reference point. All measurements were taken for 30 minutes. The four corners of the building were chosen as measurement points. Total ten accelerometers were used for the measurements. The eight accelerometers were placed in the longitudinal and horizontal directions on the surfaces of shearwalls. The one

accelerometer was placed in the vertical direction on the floor. And the reference accelerometer was placed in the longitudinal direction on the shearwall of 11th floor. The measurement setup and location of the accelerometers are given in Fig. 4.

Mounting of accelerometers and data acquisition system are given in Figs. 5-6, respectively.

a) Mounting of the accelerometers

b) Mounting of reference accelerometer

Fig. 5. Details of accelerometer mounting

Fig. 6. Data acquisition system and the connection cables

Response signals obtained from the measurements were analysed and evaluated. The modal parameters (frequencies, mode shapes, and modal damping ratios) were obtained using the Enhanced Frequency Domain Decomposition (EFDD). The natural frequencies, modal damping ratios and mode shapes were extracted from the power spectra by selecting peak values. The power spectral density function of the building obtained using the EFDD technique is depicted in Fig. 7.

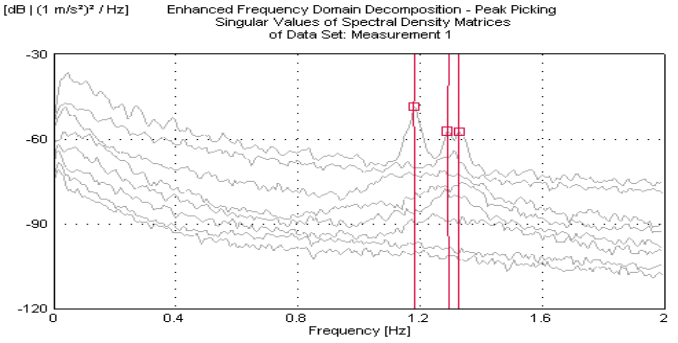

Fig. 7. The power spectral density function obtained from the EFDD technique

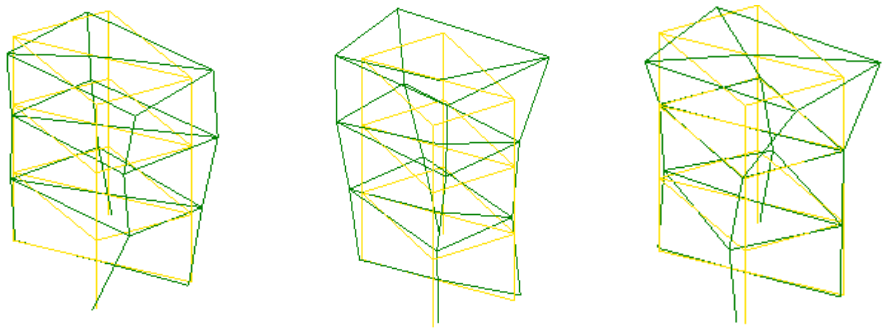

1st Mode (f_1=1.184Hz) 2nd Mode (f_2=1.296Hz) 3rd Mode (f_3=1.328Hz)

Fig. 8. The first three experimental mode shapes of the building

The mode shapes of the building determined by the EFDD technique are given in Fig. 8

The first three experimental frequencies were obtained between 1.1-1.4 Hz. The first three mode shapes of the building were obtained as torsional mode, transverse mode and longitudinal mode, respectively.

3.4. Finite Element Model Updating of the Building

When the natural frequencies and mode shapes obtained from the analytical and experimental studies are compared, it is seen that there are some differences between the results. It is thought that these differences result from some uncertainties in the finite element model of the building. Therefore, it is needed to calibrate the initial analytical model in order to determine the real behaviour of the building. For the calibration, modulus of elasticity of brick and boundary conditions were considered. As boundary condition, spring was assigned to the building base and the outer surfaces of the basement floors in order to consider the soil-structure interaction. Material properties and spring coefficients used in the updated model are given in Table 2 and Table 3, respectively. At the end of the calibration process, the experimental, initial and updated natural frequencies are presented in Table 4.

Table 2. The updated material properties of the building

Materials	Modulus of Elasticity (N/m^2)	Poisson Ratio	Density (kg/m^3)
Concrete (C30)	3.2E10	0.2	2 450
Brick	1.08E9	0.2	1 600

Table 3. The spring coefficients of the updated finite element model of the building

Boundary Conditions	Spring Coefficients (kN/m)		
	Transverse	Longitudinal	Vertical
Under the base	36 600	36 600	36 600
On the basement walls	12 200	12 200	12 200

Table 4. The experimental and analytical natural frequencies of the building

Mode Numbers	Natural Frequencies (Hz)			
	Experimental Results	Initial Model	Updated Model	Differences (%)
1	1.184	1.639	1.184	0.00
2	1.296	1.820	1.291	0.39
3	1.328	1.907	1.370	3.16

It can be seen from Table 4 that the average difference in the natural frequencies is approximately attained as 3% for the first three modes. The calibrated mode shapes are presented in Fig. 9.

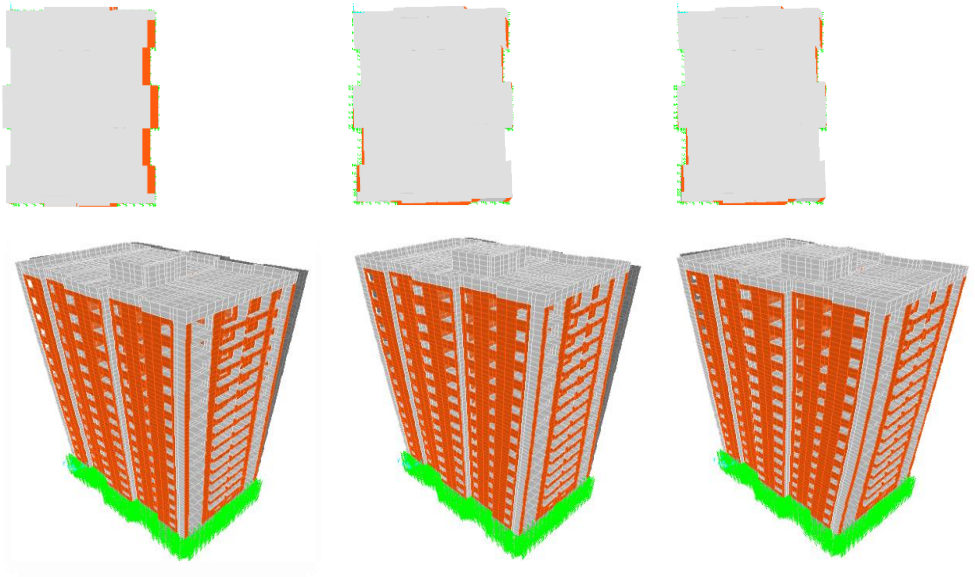

1st Mode (f_1=1.184Hz) 2nd Mode (f_2=1.291Hz) 3rd Mode (f_3=1.370Hz)

Fig. 9. The first three mode shapes of the updated building model

The first three updated analytical frequencies were obtained between 1.1-1.4 Hz. The first three mode shapes of the building were obtained as transverse mode, torsional mode and torsional mode, respectively.

It can be seen from Fig. 9 that updated mode shapes of the building have not a good harmony with experimental mode shapes. It is considered that this disharmony results from especially uncertainties about boundary conditions.

3.5. Analyses of the Building for Earthquake Motions

Duzce earthquake in 1999 as a near-fault ground motion and Imperial Valley earthquake in 1979 as far-fault ground motion were selected for the analysis. Some characteristics of these earthquakes are given in Table 5 (M: magnitude, d: distance, PGA: peak ground acceleration, PGV: peak ground velocity, PGD: peak ground displacement).

Table 5. Characteristics of the selected near and far-fault ground motions [36]

Earthquake	Record/Component	M	d (km)	PGA (cm/s^2)	PGV (cm/s)	PGD (cm)
1999 Duzce	DUZCE/DZC270	7.1	8.2	524.84	83.5	51.59
1979 Imperial Valley	IMPVALL/H-VCT345	6.5	54.1	163.83	8.3	1.05

The initial and updated analytical models of the building were analysed linearly under earthquake motions. The ground motions were applied to the building in X-axis direction (in the weak direction of the building). The relationship between height and displacements under earthquake motions is given in Fig. 10. As can be seen from Fig. 10, the displacements increase with increasing story height. In addition, it is seen that the displacements obtained from the calibrated model are bigger than these of the initial model for both far and near-fault ground motions.

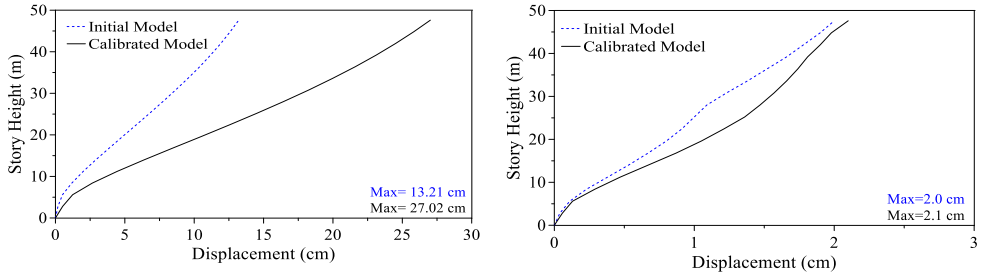

a) 1999 Duzce Earthquake b) 1979 Imperial Valley Earthquake

Fig. 10. The relationship between height and displacement under near and far-fault ground motions

Displacements, velocities and accelerations occurring on the 17th floor of the building under far and near-fault ground motions are comparatively plotted in Fig. 11. Frequency contents of displacement, velocity and acceleration obtained from the initial and the calibrated models under near and far-fault ground motions were observed to be compatible with each other.

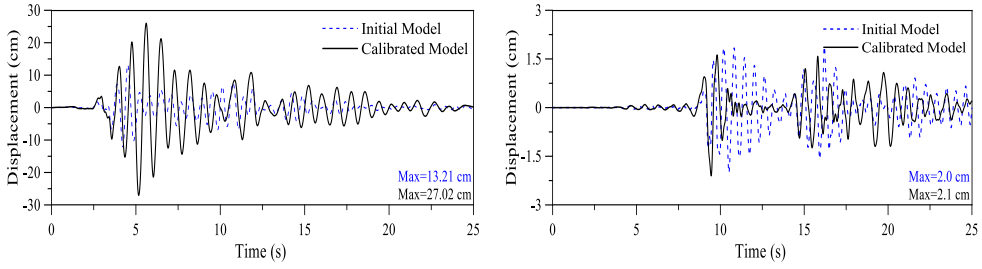

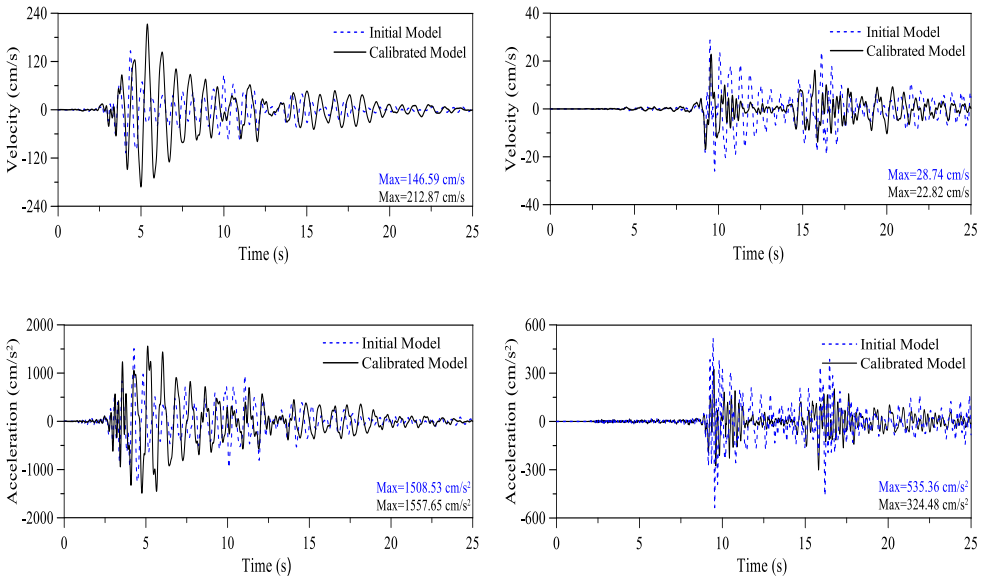

a) 1999 Duzce Earthquake b) 1979 Imperial Valley Earthquake

Fig. 11. The time histories of the displacement, velocity and accelerations on the 17th floor

Time histories of base bending moment and base shear force obtained for both ground motions are given in Figs. 12-13, respectively.

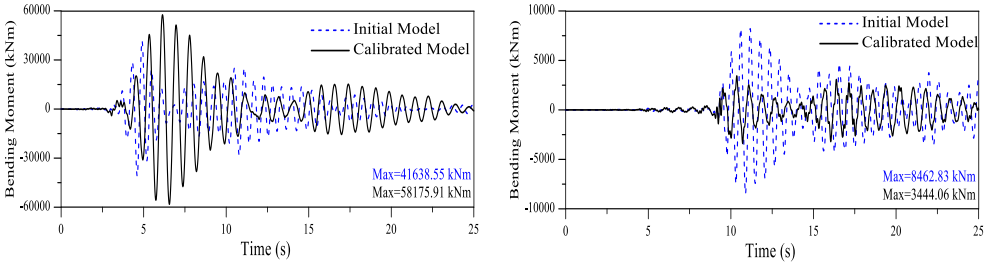

a)Duzce Earthquake b) Imperial Valley Earthquake

Fig. 12. Time histories of base bending moment for the earthquakes

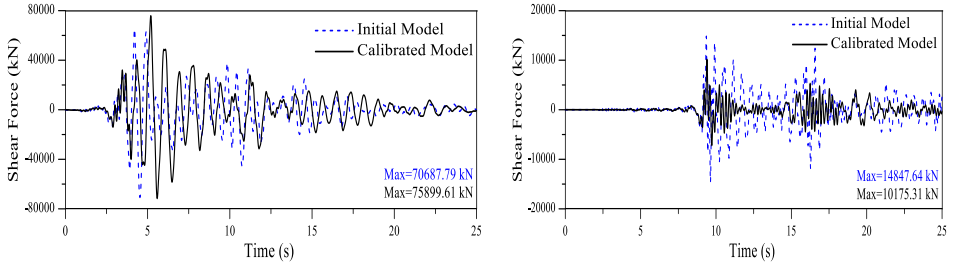

a)Duzce Earthquake b) Imperial Valley Earthquake

Fig. 13. Time histories of base shear force for the earthquakes

As can be seen from Figs. 12-13, although calibrated model increases the bending moment and shear force under near-fault ground motion, it reduces them under far-fault ground motion.

Max compressive and tensile stresses occured under the earthquake ground motions are given in Figs. 14-15, respectively.

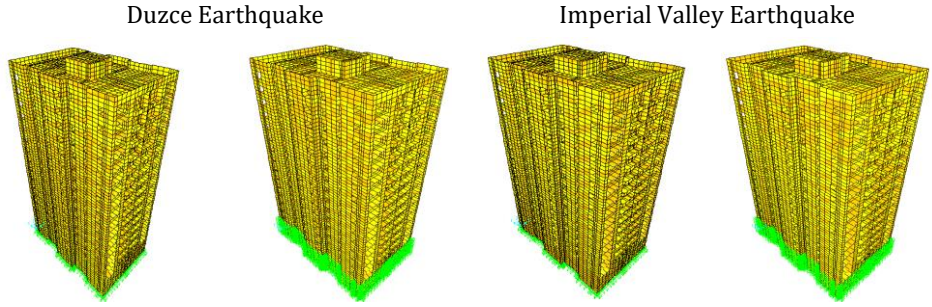

Fig. 14. Compressive stresses obtained from the earthquakes

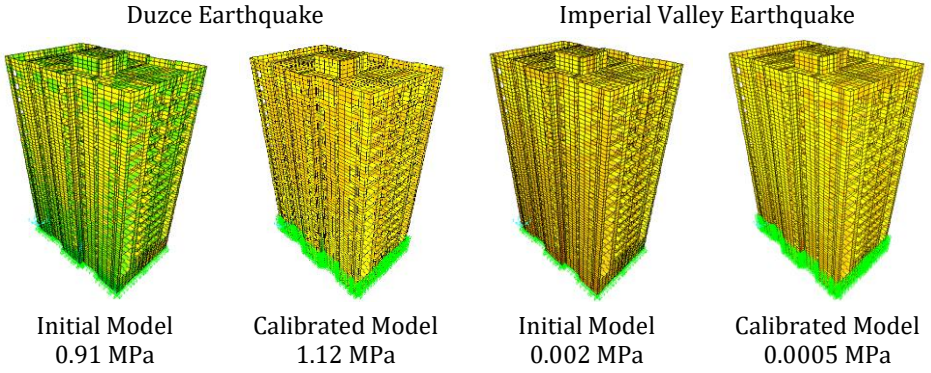

Fig. 15. Tensile stresses obtained from the earthquakes

As can be seen from Figs. 14-15, the compressive and tensile stressses increase in calibrated model under near-fault ground motion, but they reduce under far-fault ground motion.

4. Conclusions

The paper investigates the effects of ambient vibration based model updating on the seismic behaviour of a RC tall building under earthquake motions. The results obtained from the study are summarized below:

- Approximately 43% difference between the initial analytical and experimental natural frequencies of the building for the first three modes is observed. After model calibrating, the differences between calculated and experimental natural

frequencies are reduced to approximately 3%. But mode shapes have not a good harmony each other because the boundary conditions are not met exactly by the analytical model.

- Difference between displacements obtained from the initial and the calibrated models along the height of the building under the near-fault ground motion is bigger than under the far-fault ground motion.
- The displacements, velocities and accelerations calculated from the calibrated model for near-fault ground motion are generally larger than these of the initial model. However, it is observed opposite situation for the far-fault ground motion.
- Frequency contents of the displacement, velocity and acceleration obtained from the initial and the calibrated models are generally compatible with each other.
- Unlike the results of far-fault ground motion, the base bending moments and base shear forces obtained from the calibrated model for near-fault ground motion are bigger than these of the initial model.
- Max compressive and tensile stresses obtained from the calibrated model for near-fault ground motion are bigger than these of the initial model, whereas the opposite situation prevails for the far-fault ground motion. And, because the compressive and tensile stresses obtained from both the models are smaller than concrete's, the building is safe in terms of compressive and tensile stresses.

It can be generally said that the effects of finite element model updating and near-fault ground motion in the assessment of tall RC buildings must be taken into account.

References

[1] Kareem A, Gurle K. Damping in structures: its evaluation and treatment of uncertainty. Journal of Wind Engineering and Industrial Aerodynamics, 1996, 59(2):131–157. https://doi.org/10.1016/0167-6105(96)00004-9

[2] Au SK, Zhang FL. Ambient modal identification of a primary-secondary structure by fast Bayesian FFT method. Mechanical Systems and Signal Processing, 2012; 28:280–296. https://doi.org/10.1016/j.ymssp.2011.07.007

[3] Au SK, Ni YC, Zhang FL, Lam HF. Full-scale dynamic testing and modal identification of a coupled floor slab system. Engineering Structures, 2012; 37:167–178. https://doi.org/10.1016/j.engstruct.2011.12.024

[4] Au SK, Zhang FL and Ni YC. Bayesian operational modal analysis: theory, computation, practice. Computers and Structures, 2013;126:3–15. https://doi.org/10.1016/j.compstruc.2012.12.015

[5] Ventura CE, Schuster ND. Structural dynamic properties of a reinforced concrete high-rise building during construction. Canadian Journal of Civil Engineering, 1996; 23:950-972. https://doi.org/10.1139/l96-901

[6] Wu JR, Li QS. Finite element model updating for a high-rise structure based on ambient vibration measurements. Engineering Structures, 2004;26(7):979-990. https://doi.org/10.1016/j.engstruct.2004.03.002

[7] Miyashita K, Itoh M, Fujii K, Yamashita J, Takahashi T. Full-scale measurements of wind-induced responses on the Hamamatsu ACT tower. Journal of Wind Engineering and Industrial Aerodynamics, 1998; 74: 943–953. https://doi.org/10.1016/S0167-6105(98)00086-5

[8] Xu YL, Zhan S. Field measurements of Di Wang tower during typhoon York. Journal of Wind Engineering and Industrial Aerodynamics, 2001;89:73–93. https://doi.org/10.1016/S0167-6105(00)00029-5
[9] Li QS, Fang JQ, Jeary AP, Wong CK. Full scale measurements of wind effects on tall buildings. Journal of Wind Engineering and Industrial Aerodynamics, 1998;74:741–750. https://doi.org/10.1016/S0167-6105(98)00067-1
[10] Li QS, Yang K, Wong CK and Jeary AP. The effect of amplitude-dependent damping on wind-induced vibration of super tall building. Journal of Wind Engineering and Industrial Aerodynamics, 2003;91: 1175–1198. https://doi.org/10.1016/S0167-6105(03)00080-1
[11] Li QS, Wu JR, Liang SG, Xiao YQ, Wong CK. Full-scale measurements and numerical evaluation of wind-induced vibration of a 63-story reinforced concrete tall building. Engineering Structures, 2004;26(12):1779-1794. https://doi.org/10.1016/j.engstruct.2004.06.014
[12] Li QS, Xiao YQ, Fu JY, Li ZN. Full-scale measurements of wind effects on the Jin Mao building. Journal of Wind Engineering and Industrial Aerodynamics, 2007;95:445–466. https://doi.org/10.1016/j.jweia.2006.09.002
[13] Brownjohn JMW. Ambient vibration studies for system identification of tall buildings. Earthquake Engineering and Structural Dynamics, 2003;32(1): 71-95. https://doi.org/10.1002/eqe.215
[14] Boroschek RL, Yá-ez FV. Experimental verification of basic analytical assumptions used in the analysis of structural wall buildings. Engineering Structures. 2000; 22(6): 657-669. https://doi.org/10.1016/S0141-0296(99)00007-3
[15] Li Q, Yi J. Monitoring of dynamic behaviour of super-tall buildings during typhoons. Structure and Infrastructure Engineering, 2016; 12(3): 289-311. https://doi.org/10.1080/15732479.2015.1010223
[16] Liu T, Yang B, Zhang Q. Health monitoring system developed for Tianjin 117 high-rise building. Journal of Aerospace Engineering, 2016; B4016004. https://doi.org/10.1061/(ASCE)AS.1943-5525.0000602
[17] Zhang FL, Xiong HB, Shi WX, Ou X. Structural health monitoring of Shanghai Tower during different stages using a Bayesian approach. Structural Control and Health Monitoring,2016. https://doi.org/10.1002/stc.1840
[18] Li QS, Wu JR. Correlation of dynamic characteristics of a super tall building from full-scale measurements and numerical analysis with various finite element models. Earthquake Engineering and Structural Dynamics, 2004;33:1311-1336. https://doi.org/10.1002/eqe.405
[19] Pan TC, Brownjohn JMW, You XT. Correlating measured and simulated dynamic responses of a tall building to long-distance earthquakes. Earthquake Engineering and Structural Dynamics, 2004;33(5):611-632. https://doi.org/10.1002/eqe.366
[20] Chassiakos AG, Masri SF, Nayeri RD, Caffrey JP, Tzong G, Chen HP. Use of vibration monitoring data to track structural changes in a retrofitted building. Structural Control and Health Monitoring, 2005;14(2): 219-238.
[21] Archila M, Boroschek R, Ventura CE, Molnar S. Modal testing of a repaired building after 2010 Chile earthquake. In Topics in Dynamics of Civil Structures,2013;4:119-125.
[22] Pan Y, Ventura CE, Feng Y, Li X, Kaya Y, Xiong H, Zhou M. Ambient vibration testing of a super tall building in Shanghai. InDynamics of Civil Structures, 2016;2:155-162. https://doi.org/10.1007/978-3-319-29751-4_16
[23] Liao WI, Loh CH, Lee BH. Comparison of dynamic response of isolated and non-isolated continuous girder bridges subjected to near-fault ground motions.

Engineering Structures, 2004;26(14):2173–283. https://doi.org/10.1016/j.engstruct.2004.07.016
[24] Çavdar Ö. Probabilistic sensitivity analysis of two suspension bridges in Istanbul, Turkey to near-and far-fault ground motion. Natural Hazards and Earth System Sciences, 2012; 12(2):459–473. https://doi.org/10.5194/nhess-12-459-2012
[25] Dicleli M, Buddaram S. Equivalent linear analysis of seismic-isolated bridges subjected to near-fault ground motions with forward rupture directivity effect. Engineering Structures, 2007;29(1):21–32. https://doi.org/10.1016/j.engstruct.2006.04.004
[26] Liu T, Luan Y, Zhong W. Earthquake responses of clusters of building structures caused by a near-field thrust fault. Soil Dynamics and Earthquake Engineering, 2012; 42:56–70. https://doi.org/10.1016/j.soildyn.2012.06.002
[27] Mazza F, Vulcano A. Effects of near-fault ground motions on the nonlinear dynamic response of base-isolated RC framed buildings. Earthquake Engineering and Structural Dynamics, 2012;41(2):211–232. https://doi.org/10.1002/eqe.1126
[28] Mortezaeia A, Ronaghb HR, Kheyroddinc A. Seismic evaluation of FRP strengthened RC buildings subjected to near-fault ground motions having fling step. Composite Structures, 2010; 92(5):1200–1211. https://doi.org/10.1016/j.compstruct.2009.10.017
[29] Trifunac MD. The role of strong motion rotations in the response of structures near earthquake faults. Soil Dynamics and Earthquake Engineering, 2009; 29(2):382–393. https://doi.org/10.1016/j.soildyn.2008.04.001
[30] Jacobsen NJ, Andersen P, Brincker R. Using enhanced frequency domain decomposition as a robust technique to harmonic excitation in Operational Modal Analysis. Proceedings of ISMA2006: International Conference on Noise and Vibration Engineering, Leuven, Belgium, 2006.
[31] Bendat JS, Piersol AG. Random data: analysis and measurement procedures. 3th Edition, John Wiley and Sons, USA, 2004.
[32] Brincker R, Zhang L, Andersen P. Modal identification from ambient responses using frequency domain decomposition. 18th International Modal Analysis Conference, San Antonio, USA, 2000.
[33] SAP2000 (2008) Integrated Finite Element Analysis and Design of Structures, Computers and Structures, Inc., Berkeley, California, USA.
[34] PULSE (2006) Analyzers and Solutions, Release11.2. Bruel and Kjaer, Sound and Vibration Measurement A/S, Denmark.
[35] OMA (2006) Operational Modal Analysis, Release 4.0. Structural Vibration Solution A/S, Denmark.
[36]http://peer.berkeley.edu/smcat/search.html.